

## MINERALOGICAL AND CHEMICAL PROPERTIES OF EL-FAYOUM CLAYS

By

M. A. ABDEL MAKSOUH\*, B. A. SABARAH\*\* and E. A. EBIED\*\*

\*Department of Geology, Faculty of Science, University of Qatar, Doha, Qatar

\*\*Department of Chemistry and Physics, Faculty of Education, Fayoum, Cairo University

### الخواص المعدنية والكيميائية لرواسب الطين الفيوم - مصر

محمد علي عبد المقصود و برى عبد الغني صبرة و إلهام أحمد عبيد

منطقة الباتس ديمو بالفيوم بها تتابع طيني سمكه ١٧ متر مغطى جزئياً بتكوين بلايستوسين . وقد اثبتت الدراسة باستعمال الاشعة السينية ان التركيب المعدني السائد هو الاسمكتيت يليه الكاولينيت بينما توجد الطبقة المختلطة البت / اسمكتيت بكمية قليلة. وتعتبر المعادن اسمكتيت وكاولينيت الناتج النهائي لعملية تداعي . أما المحتوى الغير طيني فهو خليط من معادن الكوارتز والكالسيت والدولوميت والفلسبار البوتاسي . وتثبت حسابات النسب الاساسية للتركيب الكيميائي وكذلك طريقة توزيع العناصر في التكوين الطيني وجود تجانس تركيبى وتثبت العلاقات الكيميائية للعناصر الاساسية ان هذه الصخور ترسبت في بيئة بحرية ضحلة . ونتيجة لهذا التجانس فإن هذا التكوين يصلح للاستخدام في صناعة الحراريات .

*Key Words:* Clays, Mineralogy, Chemistry, El-Fayoum

#### ABSTRACT

El-Batts Demo Area constitutes a part of El-Fayoum province in Egypt, it is dominated by clay formations 17 meters thickness, covered in part by a thin layer of Pleistocene deposits.

XRD studies reveal that smectite is the dominant clay mineral. Kaolinite is the next in frequency. Illite and the mixed layer illite / smectite occur in minor capacities. The minerals smectite and kaolinite are the end product of degradation process. The nonclay minerals, recorded, are detrital quartz, calcite, dolomite, and K-feldspars.

The Significance of elemental ratios calculated from chemical data and the mode of distribution of the major elements are discussed. The geochemical criteria indicate a shallow marine sedimentary environment for these clays. A high degree of chemical homogeneity is detected among the examined samples.

#### INTRODUCTION

El-Fayoum depression (1700 km<sup>2</sup>) constitutes a part of the Western Dessert of Egypt. It is of circular out-lines and located just to the west of the Nile Valley, some 100 kilometers southwest of Cairo. The formation of this morphotectonic depression started structurally with streams, and wind acted on Eocene rocks of different hardness.

The stratigraphy of El-Fayoum has been carefully studied by several authors among whom may be mentioned; Beadnell (1950), Blankenhorn (1921), Sandford and Arkel (1929), Gardner (1929), Cuveillier (1930), Little (1936), Ansary (1955), Said (1962), Abdel Kareem (1971), Strougo (1977),

and Shamah (1981). Generally the rocks exposed are all of sedimentary nature, except the basalt of Gabal Qatrani which is of Oligocene age. The succession in El-Fayoum province belongs to the Eocene sediments. The rocks range from middle Eocene- lower Lutetian (El-Masaqheit section) to Upper Lutetian at Gehannem region and qarret El-Faras. At the northern part of El-Fayoum, the Oligocene and relics of the lower Miocene are exposed. At the middle part Pliocene, and Recent sediments are recorded.

The present work deals with the XRD studies and variation of the major oxides in a clay formation at El-Batts Demo area, a part of El-Fayoum province (Fig. 1). The area is traversed by a main Wadi running N-S, where a sedimentary section of

clays, and calcareous sandstone are exposed on both sides of the wadi (Fig. 2). The eastern as well as the western banks are capped by cultivated lands (formed up of silt). The clays at the wadi floor are covered in part by pliestocene deposits which in turn are overlain by cultivated land. The section is clay, approximately 17m. in thickness with 15.20 cm. of fine calcareous sandstone intercalation. Sabarah *et al.* (1985), investigated the clay section and considered it as unfossiliferous clay due to the lack of fauna record. On basis of stratigraphic correlation, structural evidence, and lithology, they assigned these clays to the marine Pliocene.

Microscopic investigations reveal that the clays show little content of K-feldspar, calcite and few quartz grains. The sandstone intercalation is dominated by well sorted angular to subangular quarts grains, cemented by argillaceous and calcareous materials. Accessories are pyroxenes and iron oxides. The pliestocene deposits at the wadi floor are generally composed of mixed gravels and sands with pebbles mostly derived from the Nubian Sandstone and the Basement complex of the Eastern Desert. The heavy mineral content of that sandstone is composed chiefly of iron oxides, biotite, epidote, tourmaline, zircon, hornblende, and garnet.

Sabrah *et al.* (1985) examined also mineralogically, and chemically two vertical sections in El-Batts Demo area, one on the eastern and the other on the western bank of the main Wadi. The study reveals vertical homogeneity for the clay where 10 samples are composed of smectite 15% kaolinite 39.7%, and illite 9.3%. In the present study, the lateral homogeneity as well as the distribution of clay minerals and major oxides are investigated to present an overall idea about the utility of that clay formation in any industrial use especially in the production of building materials such as bricks.

LABORATORY TECHNIQUES

Chemical analyses of the major elements was carried out on the clay samples collected from the eastern and western banks of the main wadi.

The apparatus used is an X-Ray Fluorescence Crystal Spectrometer. consisting of three principle sections which effects excitation, dispersion and detection and read out respectively. The measurements are made with the scalar and timer. Intensity data were converted to analytical data by comparison standard method where the analyzed line-intensity from the samples was compared with that from the standards having the same form as the samples and nearly the same analytical-concentration and matrix. Chemical data are listed in Table 2, in addition average world analyses are given for purpose of comparison.

The study includes X-ray diffraction analyses, of eight samples out of the eighteen samples, chemically analyzed. The XRD analyses are for the whole rock samples (4) and the less than 2 micron size fraction. For the latter, the selected samples were slightly crushed and representative portion of each was disaggregated by soaking in distilled water for few days followed by stirring with a high speed electric stierer. About 10 ml of 10% sodium hexametaphosphate were added to the distilled water and dispersion was finally carried out using an ultrasonic probe. Clay fraction (<2 m) was separated by setting technique based upon Stock's law (Folk, 1968). The suspension of clay fractions were allowed to settle into a Millipore Filter (Pore Size 0.2 m) under vacuum. Then, the film was transferred to glass slide by gently pressing the clay towards the glass slide and carefully removing the filter paper to produce preferred orientation of the clay minerals. Duplicate oriented slides were prepared from each sample; one slide was analyzed before and after heating to 450-550°C; the other slide was checked for expandable clay after 24 hours exposure to a saturated ethylene glycol atmosphere at 60°C (Brunton, 1955).

The X-ray diffraction analyses were performed on a phillipe Norelco diffractometer operated at 1° 20/min., Nickel Filtered Cu K -radiation generated at 36 KV and 20 mA was used. The x-ray diffractograms are shown in figure 3.

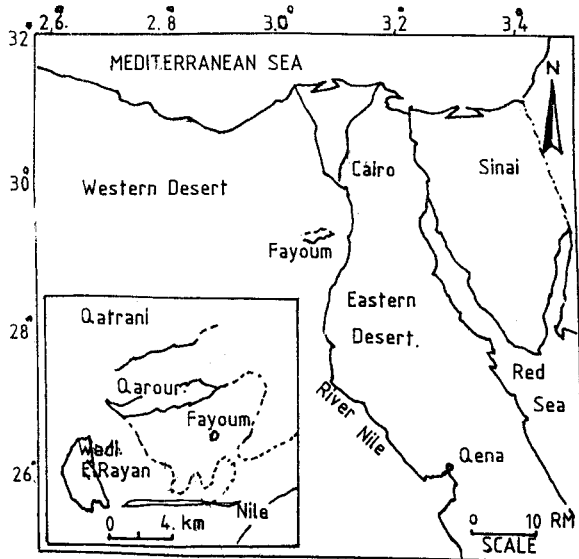


Fig. 1: Location map, showing the examined area (°).

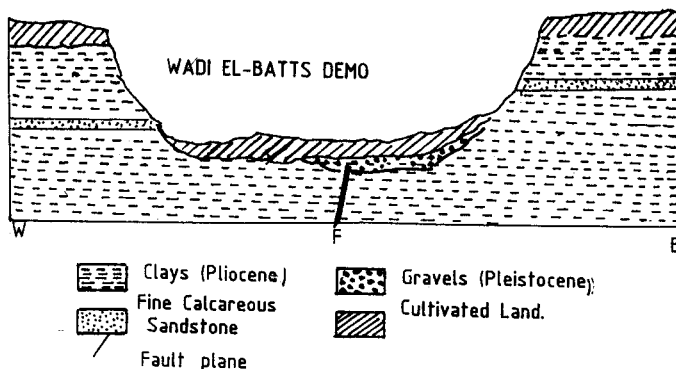


Fig. 2a: An East-West geologic cross-section in El-Batts Demo area.

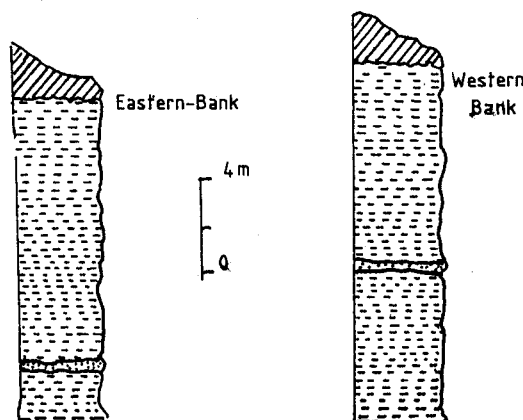


Fig. 2b: Showing two vertical sections, to the scale, on both sides of Wadi El-Batts Demo.

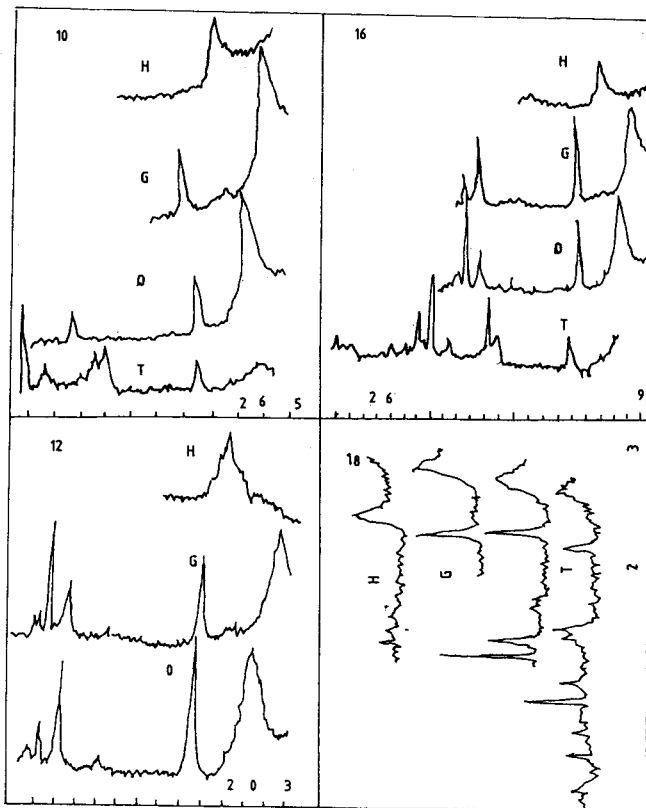


Fig. 3: x-Ray diffractograms of El-Batts Demo Clays.

The identification of clay minerals was facilitated by the use of ASTM cards, Brown (1961), and other published data. The relative percentage of expanded layer (smectite), which occurs in randomly interstratified mixed-layer minerals is determined from the position of the combined (001), (001) reflection of the mixed-layer following glycerol treatment (Weaver, 1956, and Mac Evan *et al.*, 1961). In the present work the semiquantitative relative proportions of the clay minerals were obtained by measuring the peak areas of their first order basal reflections i.e. 15 A°, and 17 A° for smectite, before and after glycerol treatment respectively, 7 A° for Kaolinite, 10 A° for illite and 12 - 13 A° for the irregular mixed layer illite/smectite, above the background (Norrish and Taylor, 1962). Weighting factors, Johns, *et al.* (1954), Weaver (1961), and Biscay (1965) were used to relate the peak area mineral to the total concentration of the mineral present. On the other hand, the nonclay minerals were generally noted as an adjacent to clay mineral identification. Consequently semiquantitative X-ray determination of them was not attempted mineralogically. Data observed are listed in Table 1.

Table 1

Compositional variation of the mineral groups in the <2µm fraction of the deposit.

d(001) A° of clay minerals and their relative Abundance						
Sample No.	Smectite	Kaolinite	Illite	Illite/Smectite mixed Layer	Remarks	
1	79.4	19.8	0.8	-		
Eastern Bank	3	76.5	22.6	0.9	-	Quartz, K-feldspar,
7	75.2	21.3	-	3.5		
9	85.2	13.8	0.3	-		Calcite, and Dolomite ar

Table 1 Contd.

Compositional variation of the mineral groups in the <2µm fraction of the deposit.

d(001) A° of clay minerals and their relative Abundance						
Sample No.	Smectite	Kaolinite	Illite	Illite/Smectite mixed Layer	Remarks	
10	91.9	7.1	1.0	-	accessories	
Western Bank	12	85.6	13.9	0.5	-	in variable amounts
16	80.5	17.2	2.3	-		
18	58.5	36.1	5.4	-		
Averages	79.2	19.0	1.4	0.4		

RESULTS

Figure 3, shows the diffractograms for eight analyzed samples. Smectite is the dominant clay mineral group while kaolinite is next in frequency.

Illite and the mixed-layer illite/smectite are in minor frequency in all samples (see Table 1). Semiquantitative data on the clay minerals indicate that smectite range between 58.5% and 91.9% with an average of 79.2%. This is followed by Kaolinite which range between 7.1% and 36.1%, giving average of 19.0%. The content of illite reaches up to 5.4% with an average of only 1.4%. Sample No. 7, contains minor amount of the mixed-layer illite/smectite (3.5%). The nonclay minerals detected from the diffractograms of the whole samples are quartz, alkali-feldspars, calcite, and dolomite. These occurs in accessory capacity but of variable proportions.

The average for major element-constituents of the studied samples are estimated and listed in Table 2. Comparing these averages with the average world analyses shown in the same table, it is evident that the analyzed samples show slight increase in silica mainly due to the presence of free quartz. Alkalies also increase slightly as some alkali feldspars are recorded in the examined samples. The structure of the feldspars contains in addition to alkalies, an equivalent amount of alumina, and three times this amount of silica. Consequently Al<sub>2</sub>O<sub>3</sub> is increased slightly with silica above the world averages. The average iron content matches well the average world data. The elemental ratios TiO<sub>2</sub>/Al<sub>2</sub>O<sub>3</sub>, Si/Al, K/Al, and Na/K are calculated and listed in the same table.

DISCUSSION

The XRD data of Table 1 indicate that the clay-minerals are essentially smectite (average of 79.2%), Kaolinite (average of 19%) and accessory illite (average 1.4%) The mixed layer illite/smectite is recorded only in one sample (3.5%). These clays are most probably originated by weathering of basement rocks and there after were transported and deposited in the present suite. The presence of high smectite, and kaolinite contents indicates that these minerals are the last stage of degradation process. As degradation proceeds smectite and kaolinite are formed at the expense of illite, the mixed-layer illite/smectite which present only as traces is the intermediate stage in degradation before the development of kaolinite, where the removal of potassium is necessary to complete degradation.

The major components in the analyzed samples are SiO<sub>2</sub>, Al<sub>2</sub>O<sub>3</sub>, Fe<sub>2</sub>O<sub>3</sub>, and Na<sub>2</sub>O. Figure 4 shows that SiO<sub>2</sub>, and

**Table 2**  
Chemical analyses of El-Batts Demo clays

Oxides	Eastern Bank (Sample No.)								
	1	2	3	4	5	6	7	8	9
SiO <sub>2</sub>	45.97	49.15	48.16	50.36	51.34	50.56	46.01	49.02	46.60
Al <sub>2</sub> O <sub>3</sub>	22.47	22.01	22.81	22.67	22.98	21.88	23.58	23.01	22.40
Fe <sub>2</sub> O <sub>3</sub>	7.28	7.16	6.98	7.03	7.41	7.03	7.80	7.73	7.26
TiO <sub>2</sub>	1.63	1.66	1.81	1.78	1.38	1.45	1.68	1.62	1.62
CaO	1.74	1.70	2.86	2.77	2.38	2.41	3.34	2.59	2.49
MgO	1.26	1.30	1.15	1.29	1.82	1.71	1.15	1.20	1.56
Na <sub>2</sub> O	5.83	4.46	4.05	3.68	0.94	2.23	3.64	3.50	4.46
K <sub>2</sub> O	1.16	1.21	1.01	1.98	0.83	0.98	1.25	1.01	1.18
SO <sub>3</sub>	0.19	0.25	0.16	0.31	0.40	0.51	0.19	0.27	0.29
Cl	2.75	2.30	1.26	1.78	1.63	1.51	1.09	1.78	2.12
L.O.I.	9.61	9.09	10.08	7.32	8.68	7.77	10.73	8.24	9.44
Total	99.89	100.29	100.33	100.96	99.79	100.04	100.46	99.97	99.50
TiO <sub>2</sub> /Al <sub>2</sub> O <sub>3</sub>	0.07	0.08	0.08	0.08	0.06	0.07	0.07	0.07	0.07
Si/Al	1.82	1.97	1.86	1.97	1.97	2.05	1.77	1.88	1.84
Fe/Al	0.43	0.43	0.41	0.41	0.43	0.42	0.45	0.44	0.43
K/Mg	1.30	1.30	1.10	2.00	0.60	0.80	1.40	1.10	1.10
K/Al	0.08	0.09	0.07	0.13	0.06	0.07	0.07	0.07	0.08
Mg/K	4.30	3.30	3.75	1.69	1.00	2.13	2.70	3.25	3.30

Oxides	Western Bank (Sample No.)									Average World		
	10	11	12	13	14	15	16	17	18	Average ages	Coarse Clay	Fine Clay
SiO <sub>2</sub>	48.50	50.64	54.42	52.70	50.65	51.36	52.70	53.65	54.06	50.49	48.07	44.61
Al <sub>2</sub> O <sub>3</sub>	22.55	22.40	22.09	21.89	23.50	22.90	18.98	20.55	22.05	22.26	18.83	18.93
Fe <sub>2</sub> O <sub>3</sub>	6.23	6.40	6.77	6.65	7.52	7.10	7.17	7.26	6.96	7.10	6.91	7.42
TiO <sub>2</sub>	1.42	1.38	1.06	1.25	1.46	1.36	1.32	1.52	1.63	1.50	0.89	0.79
CaO	3.26	2.95	2.07	2.19	2.14	2.20	3.07	2.68	2.47	2.52	4.96	6.24
MgO	1.47	1.51	1.17	1.21	2.69	2.58	1.65	1.55	1.33	1.53	3.56	3.19
Na <sub>2</sub> O	2.85	2.75	2.22	2.35	0.96	2.67	3.32	2.89	3.50	3.13	1.17	1.19
K <sub>2</sub> O	1.08	1.10	1.07	1.08	1.10	1.15	1.08	1.19	1.02	1.14	2.57	2.62
SO <sub>3</sub>	0.47	0.52	0.18	0.31	0.60	0.65	0.46	0.48	0.13	0.35	n.d.	n.d.
Cl	2.16	2.27	0.78	1.06	1.56	1.48	1.35	1.89	2.34	1.73	n.d.	n.d.
L.O.I.	9.77	8.85	8.73	9.55	8.18	7.43	8.96	6.80	10.10	8.96	10.41	12.51
Total	99.76	100.77	100.55	100.24	100.16	100.86	100.06	100.46	100.60	100.28	97.87	97.50
TiO <sub>2</sub> /Al <sub>2</sub> O <sub>3</sub>	0.06	0.06	0.05	0.06	0.06	0.06	0.07	0.07	0.07	0.07	*Average World Analyses After Beus (1976)	
Si/Al	1.92	2.00	2.18	2.14	1.97	1.99	2.46	2.30	2.17	2.01	** Ranges are;	
Fe/Al	0.37	0.38	0.40	0.41	0.42	0.40	0.41	0.48	0.42	0.42	+ SiO <sub>2</sub> : 45.47-54.42	
K/Mg	1.00	1.00	1.30	1.30	0.60	1.00	0.90	1.10	1.00	1.10	Al <sub>2</sub> O <sub>3</sub> : 18.98-23.50	
K/Al	0.08	0.08	0.08	0.08	0.07	0.08	0.09	0.09	0.07	0.08	Fe <sub>2</sub> O <sub>3</sub> : 06.23-07.80	
Mg/K	2.33	2.22	1.78	1.84	0.78	2.00	2.78	2.10	3.25	2.44	TiO <sub>2</sub> : 01.06-01.81	
											CaO: 01.70-03.34	

Na<sub>2</sub>O: 00.94-05.83, MgO: 01.15-02.69, K<sub>2</sub>O: 00.83-01.98, SO<sub>3</sub>: 00.13-00.65, and Cl: 00.78-02.75

Na<sub>2</sub>O, decrease with the increase in Al<sub>2</sub>O<sub>3</sub> while CaO, TiO<sub>2</sub> and Fe<sub>2</sub>O<sub>3</sub> increase. The antipathetical and proportional relations between these oxides, indicate that they are linked together in mineral formulae, mostly the aluminosilicate structure of the clays and feldspars. The association of iron with titanium and alumina in clay minerals was noted by Hirst (1962). The positive relation between iron and both alumina and titanium (Fig. 4) indicate that the iron is contained either in the clay minerals or the associated minor feldspars. The distribution of the major oxides SiO<sub>2</sub>, Al<sub>2</sub>O<sub>3</sub>, Fe<sub>2</sub>O<sub>3</sub>, TiO<sub>2</sub>, CaO, Na<sub>2</sub>O, MgO, K<sub>2</sub>O, and the volatiles SO<sub>3</sub>, and Cl of the analyzed samples on both eastern and western banks are shown in Figure 5. For both banks SiO<sub>2</sub>, and Na<sub>2</sub>O, oscillate reversible to Al<sub>2</sub>O<sub>3</sub>, while CaO, iron, TiO<sub>2</sub>, and MgO show positive oscillation with alumina. K<sub>2</sub>O exhibits nearly constant distribution which indicates that potassium is mainly contained in the structure of an accessory mineral, mostly the alkali feldspar. The volatiles SO<sub>3</sub>, and Cl show similar variation trends. Consequently, the increase in SO<sub>3</sub> is expected with increase in Cl content. It is also clear from the distribution diagram of Figure 5, that all elements oscillate more or less gently around their averages which reflects to great extent, homogeneity in the chemical characters of the examined clays.

The elemental ratios TiO<sub>2</sub>/Al<sub>2</sub>O<sub>3</sub>, K/Mg, Si/Al, K/Al and Na/K, of the examined samples show ratios milling around their mean values (Fig. 6) i.e. for the same elemental ratio, samples show nearly similar values. This may be explained on basis of chemical homogeneity of the examined clays.

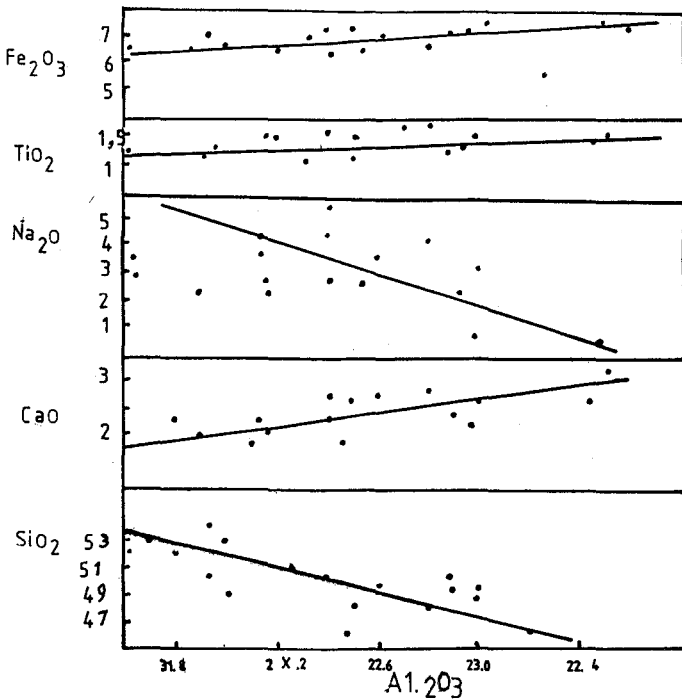


Fig. 4: Relations between the major oxides Al<sub>2</sub>O<sub>3</sub>, and SiO<sub>2</sub>, CaO, Na<sub>2</sub>O, TiO<sub>2</sub>, and Fe<sub>2</sub>O<sub>3</sub>.

The element titanium enters the crystal of the aluminosilicates of the parent rocks. On weathering it liberates with alumina and pass into colloidal state. Latter on, it enters with silica into the clay minerals. According to Goldschmidt (1945), Ti of hydrolysaltes is present as very finely crystalline TiO<sub>2</sub> (or TiO<sub>2</sub> hydrate) deposited along with the tiny flakes of

the clay minerals. TiO<sub>2</sub> shows positive correlation against Al<sub>2</sub>O<sub>3</sub> in figure 4, and the ratio TiO<sub>2</sub>/Al<sub>2</sub>O<sub>3</sub>, (Table 2) is almost constant which indicate that titanium enters into the clay mineral structure of the investigated rocks. The average Si/Al ratio is 2.01, partially lower than the value 3 for argillaceous sediments (Krauskopf, 1967). This is due mainly to high deficiency in the free quartz content of the examined samples. From Table 2 the average Fe/Al ratio is 0.43 closely resembles 0.5 giving by Krauskopf (1967) for the shales. This indicates that the iron reported is residing in the alumino-silicates (exclusively are clay minerals). This result was previously confirmed from the proportional relationship between iron and TiO<sub>2</sub> and Al<sub>2</sub>O<sub>3</sub> (Fig. 4).

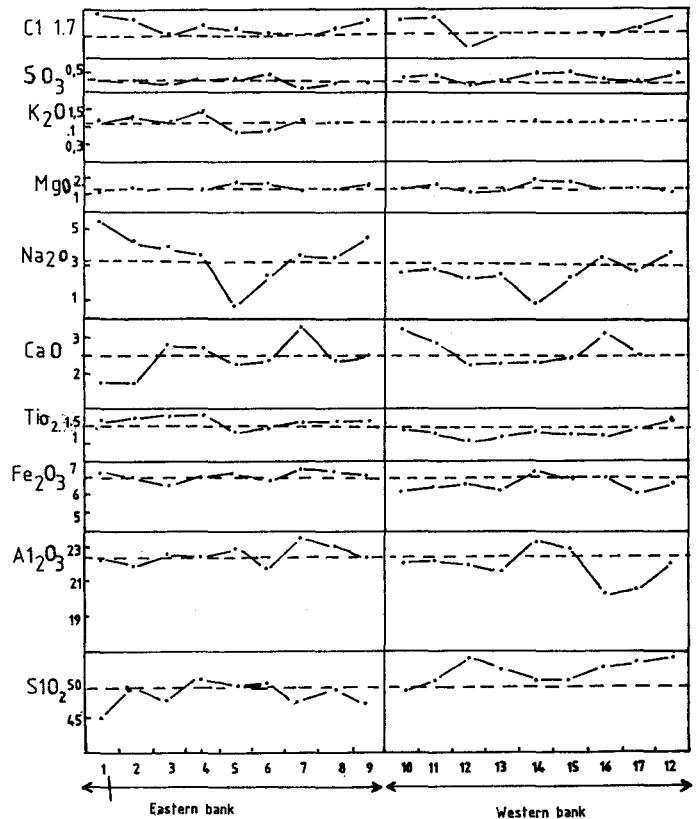


Fig. 5: The distribution of the major oxides in El-Batts Demo area. Dashed lines are the mean values.

The average K/Mg, and K/Al ratios are 1.72, and 0.29 respectively (Krauskopf, 1967). Once Mg is held mainly in the clay structure (in the present case, it is also contained in the structure of the accessory dolomite), while K, and Al are partitioned between the clay mineral- content, and the minor K-feldspar content, and as the clays are finer than both dolomite and K-feldspars, it follows that fine-grained argillaceous sediments are of higher Mg/Al and lower K/Mg ratios than coarse-grained equivalents. The estimated K/Mg ratio of the examined clays is 1.10 which is slightly lower than the average quoted for fine-grained argillaceous sediments (1.72). This suggests a relatively lower content of illite and K-feldspars, a phenomenon confirmed also by the low K/Al average ratio for the same samples (0.08), if compared with the average ratio for shale (0.29).

The Na/K ratios show an average of 2.44 which is fare above the value quoted by Rankama and Sahama (1950) for agrillaceous sediments. The presence of sodium as component-element, in intersheet positions, of the dominant clay mineral group, the smectite, and the degradation of illite,

a process usually associated with the removal of potassium, in addition to the minor occurrence of K-feldspars; are all explanations for the high Na/K ratios of the examined clays.

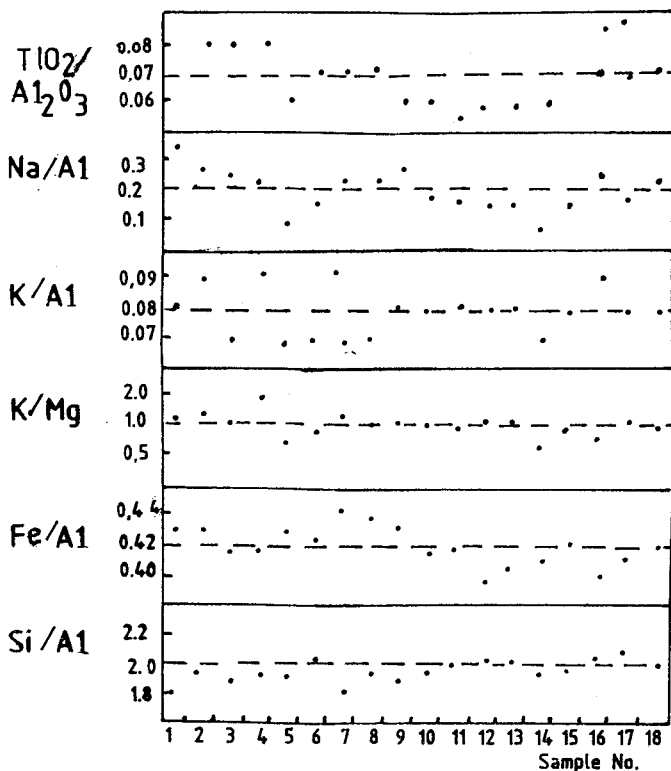


Fig. 6: Elemental ratios for El-Batts Demo clays. Dashed Lines are mean values.

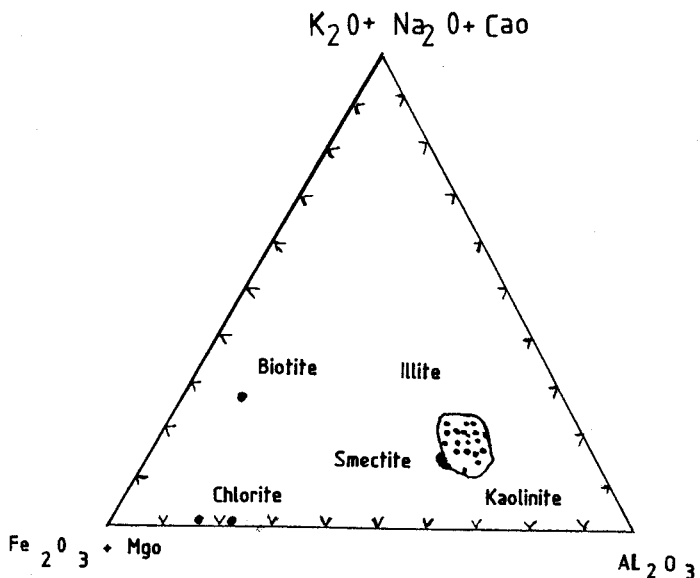


Fig. 7: Triangular relation between  $K_2O + Na_2O + CaO$ ,  $Fe_2O_3 + MgO$ , and  $Al_2O_3$  after Deer, Howie and Sussman (1966).

The ternary relation between  $K_2O + Na_2O + CaO$ ,  $Fe_2O_3 + MgO$ , and  $Al_2O_3$  is shown in Figure 7. The diagram is after Deer, Howie, and Sussman (1960). The plots of El-Batts demo clays cluster mainly around the smectite composition, which is in harmony with the XRD diffractograms of Figure 3, and their interpretations shown in Table 1.

Figure 8 is a ternary diagram with  $SO_3$ , Cl, and all other components of the sample at the three corners. It is evident that the volatile components of the examined samples ( $SO_3$  and Cl) does not exceed the line 5%. The chemical data of Table 2 show an average Cl content 1.73% which is 4.94 times as much as the  $SO_3$  average (0.35%).

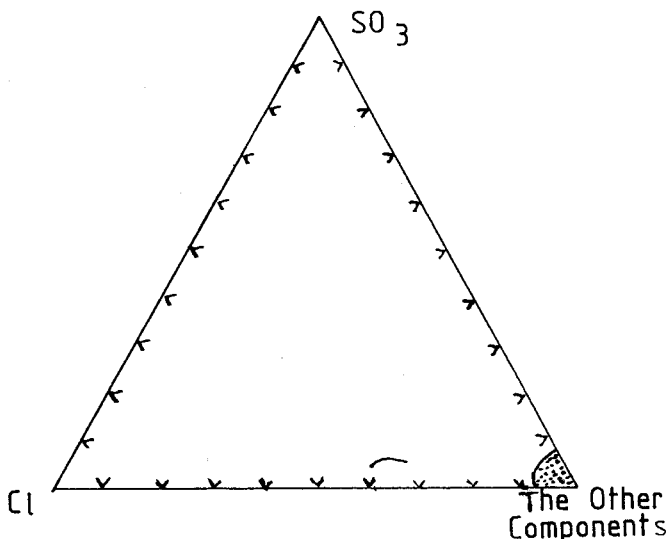


Fig. 8: Ternary relation between  $SO_3$ , Cl, and the other component-elements of El-Batts Demo clays.

The most important feature of the minerals is their excellent cationic property (mostly  $Ca^{2+}$ ,  $K^{2+}$ , and  $Na^+$ ), according to Ross and Hendrix (1945), these exchange cations (outer bases), although they enter into the composition of the montmorillonite (smectite) minerals, don't take part in their crystal structure. Upon adsorption they only serve to balance the residual negative charge of the structure develops as a result of the replacement of high-valent cations by low-valent ones e.g.  $Al^{3+}$  by  $Mg^{2+}$  in octahedral layer and  $Si^{4+}$  by  $Al^{3+}$  in tetrahedral layer. The variation between the three components K, Na, and Ca is investigated in Figure 9. From the diagram, it is clear that the field delineating the plots of the examined samples' is extending parallel to the Na-Ca base, referring to reciprocal changes between sodium and calcium while the role of potassium is mostly insignificant. It is worthy to mention that a part of the calcium content is used in the accessory calcite and dolomite which are associated with the examined clays (see Table 1). The increase of calcium at the expense of sodium initiates a reversible relationship, clearly observed in Figure 4. It is also clear from Figure 5 that the  $Na_2O$  curve oscillates reversibly to the CaO curve, while the potassium curve is fairly horizontal.

To investigate the environmental conditions prevailed during the deposition of El-Batts Demo clays, the chemical data of Table 2 were plotted on the triangular diagram Al, Fe, and (Mn + Ti) of Goldberg and Arrhenies (1958), Figure 10, where the examined clays plot within the field of the shallow marine sediments.

### CONCLUSION

The examined clays are formed by weathering and transportation of basement rocks, throughout degradation process, necessitating the removal of potassium. The intermediate stage, illite-smectite is scarcely recorded.

The antipathetical relations between  $SiO_2$ , and  $Na_2O$  and  $TiO_2$ , the proportional increase of CaO and titanium dioxide

indicate that these oxides are linked together in a mineral formulae, mostly the alumino-silicate structures of the clays, and feldspars. Iron has found to be contained in the clay structure as it increases proportionally with both  $Al_2O_3$ , and  $TiO_2$ . The lateral distribution of the major elements among the clay formation, show gently oscillation around the established averages. In addition, the elemental ratios  $TiO_2/Al_2O_3$ ,  $Si/Al$ ,  $K/Mg$ ,  $Fe/Al$ ,  $K/Al$ , and  $Na/K$ , exhibit the same property, which indicates chemical homogeneity of the examined clays. The comparison of the estimated elemental ratios with the averages calculated by Rankama, and Sahama (1950), and Krauskopf (1967), interpret well in the light of the mineralogical composition. A cationic exchange is detected between Ca, and Na, while the role of K is insignificant.

The examined clays are dominated by the smectite composition as indicated from both chemical and XRD data. Furthermore, the geochemical criteria refer to a shallow marine depositional environment for that fairly homogeneous clays.

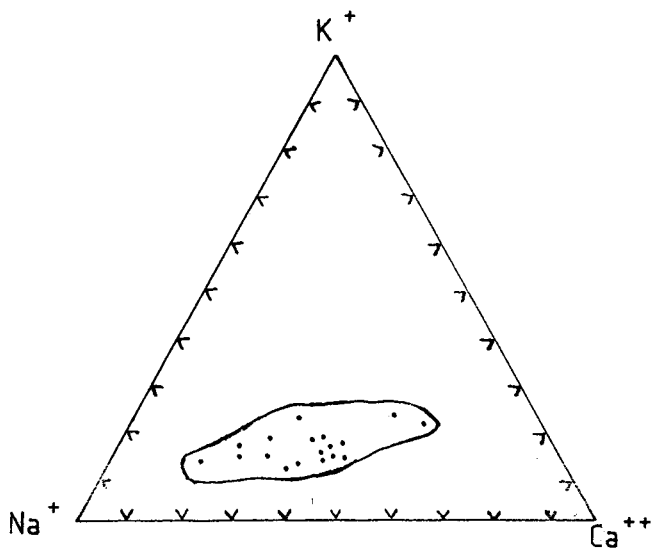


Fig.9: The plot of El-Batts Demo clays on the ternary diagram K, Na, and Ca.

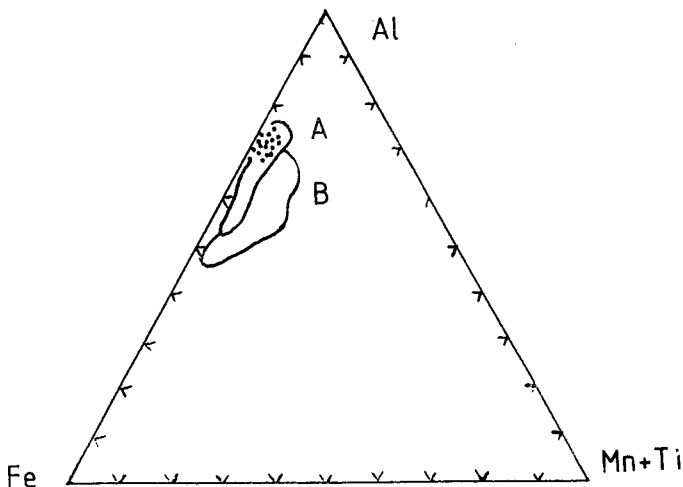


Fig. 10: Triangular Diagram for Al, Fe, and Ti, after Goldberg and Arrhenius (1958).

REFERENCES

**Abdel Kareem, M. R., 1971.** Biostratigraphic studies of some Eocene and Oligocene sections in the Fayoum province, Egypt. M.Sc. Thesis, Alexandria University.

**Ansary, S. E., 1955.** Report on the foraminiferal fauna from the Upper Eocene of Egypt. Bull. Inst. Desert, Egypt, 6: p. 160.

**ASTM 1960.** American Society for testing materials. Index to X-Ray power data file. Publication 48-1.

**Beadnell, H. J. L., 1965.** The topography and geology of the Fayoum province of Egypt. Surv. Dep. of Egypt., p. 101.

**Beus, A. A., 1976.** Geochemistry of the lithosphere. MIR Publisher, Moscow, p. 336.

**Biscaye, P. E., 1965.** Mineralogy and sedimentation of recent deep sea clay in the Atlantic Ocean and adjacent seas and oceans. Geol. Soc. America. Bull., 76: 803-832.

**Bishary, Y. 1966.** Studies on the large foraminifera of the Eocene (the Nile Valley between Assiut and Cairo and South-West Sinai), Ph.D. Thesis, Alexandria University.

**Blankenhorn, M., 1921.** Handbuch der regionalen geologie, Agypten. Carl-winters Univ., p. 244.

**Brown, G. R. (Ed.), 1961.** X-Ray identification and crystal structure of clay minerals. Miner. Soc. London.

**Brunton, G., 1955.** Vapour pressure glaucolation of oriented clay minerals. Amer. Min., 40: 124-126.

**Cuvillier, J., 1930.** Revision du Nummultique egyptien. Mem. Inst. Egypt, pp. 16, 25.

**Deer, W. A., R. A. Howie and J. Zussman, 1966.** Rock forming minerals., V.3. Sheet Silicates, Langmans, London, p. 528.

**Folk, R. L., 1968.** Petrology of sedimentary rocks. Hamphill's, Austin, Texas, p. 154.

**Gardner, E. W., 1929.** The origin of the Fayoum depression, a critical comments on a new view of its origin. Geograna Jour., 74: 371-383.

**Goldberg, E. D. and G. O. S. Arrhenius, 1958.** Chemistry of Pacific pelagic sediments. Geochim. Cosmochmi. Acta., 13: 153-212.

**Goldschmidt, V. M., 1954.** Geochemistry. Oxford University Press. London, p. 730.

**Grout, F. F., 1925.** Relation of the texture and composition of clays. Bull. Geol. Soc. Amer., 36: 393-416.

**Hirst, D. M., 1962.** The geochemistry of modern sediments from the Gulf of Paria 1. The relationship between the mineralogy and the distribution of major elements. Geochim. Acta, 26: 309-334.

**Johns, W. D., R. E. Grim and W. F. Bradly, 1954.** Quantitative estimation of clay minerals by diffraction methods. Petrol., 24: 242-251.

- Krauskopf, K. B., 1967.** Introduction to geochemistry. McGraw Hill Co., Inc., New York, p. 721. Little, G. H. 1936. recent geological work in the Fayoum and adjoining portion of the Nile Valley. Bull. Inst. Desert. Egypt, 18: 201-240.
- Mac Evan, D. M. C., A. A. Kuiz and G. Brown, 1961.** Interstratified clay minerals, X-Ray identification and crystal structure of clay minerals. 2nd Ed., ch., XI. Miner. Soc. London, pp. 393-445.
- Norrish, K. and R. M. Taylor, 1962.** Quantitative analysis by X-Ray diffraction. Clay Miner. Bull. Harper and Brothers, New York, p. 768.
- Rankama, K. and Th. Sahama, 1950.** Geochemistry. Chicago University of Chicago Press, p. 912.
- Sabarh, B. A., A. T. Abdel-Hammeed, K. M. Shamah and E. A. Ebied., 1985.** The mineralogy and geochemical characters of some clay deposits in Egypt. Refrattari e Laterizi. Faenza-Editrice Italy, 76: 186-191.
- Said, R., 1962.** The geology of Egypt. Elsevier Publ. Co., p. 377.
- Sandford, R. D. and W. J. Arkell, 1929.** Paleolithic man and the Nile-Fayoum divide. Chicago University, Orient Inst. Publ., p. 77.
- Shamah, K., 1981.** Le Paleogene de la Province du Fayoum, Egypt. Mem. Sc. de la Lerne, Paris, No. 81-31, 383 p.
- Stroguo, A., 1977.** Le Biarrizien et le Priabonien en Egypt et leurs faunes de Bivalves. These Doct., Unive. Paris, Paris-Sud, Orsay, p. 247.
- Weaver, C. E., 1956.** The distribution and identification of mixed-layer clays in sedimentary rocks. J. Miner. Soc. of Amer., 41(3 & 4): 202-221.
- Weaver, C. E., 1961.** Clay mineralogy of the Late Cretaceous rocks in the Washakie basin. Gui. book, Wyoming Geol. Assoc. 16th Ann. Conf., pp. 148-154.